CERN - PS 50 MeV LINAC PROGRESS REPORT

C.S. Taylor, J. Huguenin, F. Block, F. Chiari, P. Têtu

European Organization for Nuclear Research

Geneva, Switzerland

Introduction

The high-gradient pre-injector ($\bar{E}$ = 4.5 MV/m) has been operating with the 50 MeV linac and the PS for a period of 2 years. In this paper we describe the operational behaviour of the ion source and accelerating tube. The behaviour of the beam in the 50 MeV accelerator is then discussed in the light of recent experiments. Finally a brief account is given of the state of beam-loading compensation, and of plans for the future compensation of long beam pulses required by the PS Improvement Programme.

Pre-injector

Duoplasmatron Ion Source

Some modifications to the duoplasmatron ion source [1] have been carried out since its installation in 1966 in the interest of beam stability and ease of setting-up.

Intensity oscillation. The oscillations in beam intensity which were observed during development and early operation were found to be sensitive to the magnetic field in the region between the snout and the expansion cup, the amplitude of oscillation diminishing with increased field. In order to increase this field without too much disturbance to the field in the expansion cup itself, an additional coil was installed as shown in dashed line in Fig. 1. With 350 turns and 100 mA the original field distribution (curve a) is modified to the distribution shown by curve b (The coil is 8 mm long by 12 mm int. diam., 24 mm ext. diam., with a wire diameter of 0.3 mm). Some increase in magnetic field was also obtained by heat treatment of the anode and snout (an 11% increase for a main magnet current of 5 A).

Extraction. After a few months' running it was found that the best results from the Linac were obtained with the source set up for a 500 keV beam current of 600 mA. If the extraction voltage is adjusted to the value of 65 kV predicted by the Child-Langmuir law (for a proton current of 750 mA allowing for a 80% grid transparency, and a current density of 0.238 A/cm for R = 1 cm) the other parameters of the source can then be trimmed to obtain an optimum beam.

The extraction grid, originally of 0.1 mm diam., molybdenum wire, was replaced by vacuum heated tungsten wire about a year ago as the molybdenum melted through on several occasions.

Arc-Pulser. In order to increase the beam pulse length for multi-turn injection work, the secondary winding of the output pulse transformer has been backed off with a DC negative bias current of 1 A, which permits the pulse to deliver 1600 V for firing and a maximum current of 100 A during a 70 μs pulse.

Cathode. The technique of cathode manufacturer has been slightly modified by the addition of 0.5% collodion (in the form marketed as Colloxylinum) to the emissive mixture described in [1]. This results in a more uniform distribution of oxide on the nickel support and reduces the deposition of oxides on the snout and of barium oxide traces in the accelerating column. The normal cathode life is about 2,200 hours. Every 500 hours the emission conditions are checked by measuring the arc voltage increase for a given decrease in heater current, changing the cathode when the voltage increase passes a certain limit.

Hydrogen Pressure. The pressure in the discharge chamber is 2.3 Torr, measured with a Leybold Thermotron III, a Pirani type gauge which can work from 800 down to 10^{-2} Torr. We have used this gauge to control a needle valve, keeping the pressure to within 0.1 Torr in the snout.

Cleanliness. The presence of hydrocarbons in the pre-injector is the main cause of instabilities in the ion source beam. These impurities are particularly annoying because they appear to be deposited on the cathode when the source is not operating (there is no valve between the source and column) and are then cracked during de-gassing, forming a carbon layer which lowers the emissivity of the cathode. (See below)

Reliability. In the two years of operation of the source, the time lost due to ion source faults has been 0.3% of the total operating time.

Behaviour of the Pre-injector Accelerating Tube.

The general HT behaviour for those 2 years of operation is described in Fig. 2. The rate of loss of conditioning [2] at the beginning or at the end of each run (a run lies between 2 to 3 weeks), the weekly mean breakdown rate and some typical maximum values of cathode current are plotted. After a good start, year 1966 ended with a definite impairement : the breakdowns rate reached mean weekly values of 10 per hour with enormous peaks of 30 ÷ 100 per hour. In the meantime cathode currents which are usually zero apart from the conditioning period, went up to 2 to 5 μA for hours, which is a clear sign of pollution in the vacuum. Curiously enough, the deconditioning rate during this period was very good, as well as the breakdown rate without hydrogen at the beginning of the run before the source was started. Looking more closely at the evolution of hold-off along a normal run, one could see that the start was good but the conditions degenerated in a few days and were worse during the second half of the run. The pollution seemed to be connected with the accumulation of the operation time. A series of tests was started, trying to trace the origin of this behaviour, but no clear clue was obtained. The situation changed completely after the shut down 1967 and excellent working conditions have been obtained since then.

During the shut down the tube was dismounted (Fig. 3, 5) and inspected :

1. The titanium alloy electrodes were as usually covered with a very thin film of deposit. Typical craters were found on the maximum field regions of negative electrodes, i.e. on the cathode and the median electrode (Fig. 6). These marks were partly removed by polishing and the electrodes cleaned with our usual procedure [1]. In addition, whitish traces were found on the median electrode and on the anode pumping holes. A chemical analysis revealed that these contained barium oxyde and nickel clearly coming from the source cathode (see above).

2. The internal surfaces of the tube porcelains showed absolutely no trace of tracking or deposit (Fig. 4). Only the last porcelain on the earth side, the shielding of which for geometrical reason was not complete, had some yellowish spots in front of the cathode pumping holes : low energy secondary electrons could hit these regions, polymerizing organic films or colouring porcelain impurities. Since then, a special shield of this section has been incorporated.

3. As mentioned above the molybdenum extractor grid was found to be melted through (with a loose wire pointing towards the main 500 kV gap).

During the same shut down, the water cooling system of the Hg pumps was made more efficient, the leak rate reduced such that the pressure with source off went from 2.10^{-6} to 2.10^{-7} Torr. Regular degassing of the N_2 cold traps was started at this period too (1 trap is degassed every 3rd week), the liquid N_2 filling system made still more reliable, and the liquid N_2 dewars were pressurized with N_2 gas instead of compressed air to prevent ice forming in the system.

The improvements after the shut down may have resulted from those changes although this cannot be known for certain. Since then the breakdown rate has reached values as low as 0.04 per hour for one week, the cathode current remains at zero and the deconditioning rate at the start of the run varies from 2 to 5 kV/h.

The main source of bad HT behaviour have already been listed in [1]. In addition the effect of improper setting of source parameters, letting the beam hit the median electrode or the cathode, was to produce breakdowns. New electrodes in the vacuum also worsened conditions for a few days after their installation. It has been shown that good working has been sometimes obtained with one pump only, if sufficiently clean and with a good speed.

A new technique of HT conditioning has been started in January 1968 with the source oxide cathode left hot (950°C) instead of cold : this prevents pollution of the oxide cathode during the high voltage formation.

Beam Measurements

A large proton beam current within a small radial emittance (or a high phase-space density) is clearly of interest at all points in an accelerator as it can result in economies in magnet apertures, keep beam losses and induced activity low, and bring direct advantages to the experimenter. Developments in pre-injectors have recently produced the new situation of there being available higher phase-space densities from the pre-injector than can be exploited in the rest of the accelerator. For example the 4-fold increase in pre-injector density which followed the installation of the duoplasmatron/high gradient column assembly at CERN in 1966 resulted in only a 2-fold increase in 50 MeV density [3]. After two years of operational observation and machine measurement the reasons for this limitation are somewhat clearer, and we shall attempt to summarize here the main points which have emerged.

We recall that the transverse behaviour of the beam was described in previous papers in terms of the 'density curve', which is a curve of the quantity of current contained within equi-density contours plotted against the emittance area within the contours . In the present state of instrumentation one can but speculate about where a given particle lies within the 6-dimensional hypervolume, and the only experimental evidence which we can obtain is the distribution of charge across the two transverse projections, i.e. the horizontal and vertical phase spaces. The density curves which we measure correspond generally to a Gaussian distribution across these phase spaces [3]. Another experimental observation is that the removal of outer phase space from one projection by aperture

limitation reduces the density over the whole of the other projection [3].

The last point is of some practical importance. One tends to suppose that the outer regions of phase space are of little consequence because of the Gaussian distribution, and that they can be trimmed away to leave the dense core of the beam intact, whereas of course the effect on the other plane can be appreciable as may be seen from the simple construction of Fig. 7. The conclusion is that is one wishes to make the full pre-injector density available at the Linac input, the maximum beam excursions must lie well within the aperture of the beam transport and matching channel. This is not the case in the present 500 keV channel, and the consequences are particularly noticeable when the beam is bunched. In combination with the emittance increase already described [3] the increased space charge forces and radial excursions produce serious beam loss between the buncher and Linac, resulting in the measured density decrease seen in Fig. 8. This incidentally causes the Linac performance to be more vulnerable to pre-injector and 500 keV misalignments than was previously the case and is thought to be one of the principal causes of the intensity deterioration in 1967. The same argument applies to the progress of the beam from the input of the Linac onwards. If the density curve is still rising at the Linac acceptance limitation point (or the beam 'fills the aperture') the density available for longitudinal trapping and acceleration will be less than that measured at the input.

From this point of view therefore we should be better off with increased beam transport apertures and a bigger Linac acceptance (one of the rewards to be gained from higher energy injection [4]).

A further practical implication is that if one is trying to investigate horizontal-vertical-longitudinal coupling effects experimentally using the density changes in one plane as an indication of coupling, great care must be taken to prevent beam loss from dominating the results. In a series of measurements which we carried out on 50 MeV densities as a function of beam emittance and intensity at 500 keV we found that at low 500 keV intensities there was a greater inequality of 50 MeV densities for unequal 500 keV emittances than a higher intensities, which may be due to a space-charge coupling effect or may be due to greater radial excursions caused by space charge which increase the beam loss in both planes and tends to equalize the 50 MeV densities at high current. Similar caution has to be exercised in the 'first-turn' density measurements which we are carrying out in the PS and in the 'drift-space' measurements.

In the latter measurements we are trying to establish whether non-linear space charge coupling produces any detectable density changes at present intensities and energies. We should like to carry out such a measurement using only a drift space and crossed slits for density measurements in order to eliminate the imprecisions concerning the effects of focusing lenses, but so far we have only been able to make a measurement involving a lens between the measuring points and slits and lenses for the density data. The procedure was to limit a 10 MeV beam in the vertical plane so that beam loss between the two measuring points separated by 24 m occurred only from excursions in the horizontal plane, The density at the centre of the horizontal plane, which should be unaffected by the loss of outer particles, was then measured at the two points and was found to have decreased by 10% in 24 m. With a 50 MeV beam on the other hand there was no detectable difference after 24 m. We are treating this result ourselves with some reserve until the measurements can be repeated at different energies a number of times (it is possible to drift a useful amount of 500 keV beam through the Alvarez structure by lowering the focusing throughout).

Returning to the limitations in the present Linac, the debunching effect of space charge at 500 keV obviously makes a contribution to the reduced trapping efficiency at high currents in addition to the radial effects already discussed. There seems nothings that one can do to the present machine at the moment to improve matters and one looks rather to the theoretical studies [5], higher energy injection [4] and the 3 MeV model studies [6] for improvements in this direction.

In addition to the low trapping efficiency there is the question of 'blow-up' or the increase in the momentum normalized emittance $\frac{\text{Area}}{\pi}\beta\gamma$ in passing from 500 keV to 50 MeV. This is not considered to be of great practical importance for present performance as it may only be responsible for a few mA of beam loss, or a few percent in density, but evidently where specifications call for time-averaged limits of a few nA/m in projected linacs the problem is of more interest.

Firstly we have demonstrated the gross properties of the focusing channel represented by the quadrupoles of Tanks II and III by measuring the overlapping of emittance at the output for separated emittances at the input (Fig. 9) with a 10 MeV beam. Tanks II and III were then restored to the accelerating conditions and the output emittances remeasured (Fig 10). Our previous measurement showed that the phase density of the beam core was not measurably affected by acceleration above 10 MeV (except for the most intense beam currents) whereas there was some non-Liouvillean behaviour (in two dimensions) above 10 MeV in the less dense regions [3]. The present results show that this is not all due to RF effects but that the passage of the beam through the focusing channel alone produces some 'smearing' of emittance [7], [8].

RF System

A system of beam loading compensation using two RF feeds per tank [3] has been in operation on the 50 MeV machine for two years, but due to a shortage of drive power we have not yet been able to exploit the full possibilities of the system. With the beam current reduced to 50 mA however we can achieve practically 100% compensation in the three tanks, and Fig. 11 shows the resulting field variations in Tank I in the vicinity of the beam pulse (at 10 μsec/cm).

The upper trace represents the signal from a wall loop at the 10 MeV end, next to the compensating RF feed loop, and the lower trace the signal from the 500 keV end, remote from the feed loop. The field during the beam pulse is very nearly flat in both cases, but it is possible to detect a slightly greater fall in field at the 500 keV end, resulting probably from the acceleration in the early gaps of particles which later fall out of longitudinal stability. One may also observe a slight 1 MHz ripple caused by the excitation of the TM_{011} mode. Both effects are visible also on the derivative signals shown in Fig. 12. In Tanks II and III, by contrast, the ripple is less pronounced although the tanks are longer. This is due to the compensating feed being at the mid-point in Tanks II and III where the TM_{011} mode is only weakly excited. In Fig. 13 we see the Tank I loop signals again, this time for the full pulse length (at 50 μs/cm) with the compensation pulse adjusted to compensate 50 mA of beam, but without the beam. In this condition there is roughly a 1 : 1 ratio of compensation power to tank dissipation.

The phase of the two Tank I wall loops was also scanned through the beam region by the gated Lissajou figure method, and one found that the compensating pulse produced a linear pulse change of between 0.1 and 0.25 $^{\circ}/\mu$s, depending on the exact setting-up of the amplifier output circuit, whereas the beam itself produced no detectable change.

With regard to the shortage of drive power for complete compensation at higher intensities, it is proposed to relieve this problem by installing a new 5 MW tube, the TH 516, in the drive system. This has been developed by the manufacturers from the TH 515 and is practically a plug-in replacement but has a higher gain.

The next major problem will be the re-design of the RF system for the 100 μs - 2 pps beam pulses required by the booster synchrotron. We propose to use a delay line modulator for the compensating anode pulse as at present, but to achieve regulation of the power output for varying beam pulse lengths and amplitudes by feed-back from the tank level to the grid bias of the compensating amplifier. This method has the disadvantage that the modulator sees a varying load as the grid bias is altered, but it is probably cheaper and simpler to attenuate this effect by throwing away power in an addition shunt resistive load than to invest in hard-tube modulators. This system will be developed on the 3 MeV model first, as will various new systems such as digitally-controlled stepping motors for tuner and phase-shifter adjustement.

Conclusions

The new pre-injector has been reliable in operation, so that an electric field gradient of 4.5 MV/m in a short accelerating tube can be said to be operationally feasible even in the presence of a half ampère proton beam. It seems clear that bigger apertures at injection energy would enable us to take better advantage of the high pulse-space density produced by this pre-injector.

Acknowledgements

We wish to acknowledge our indebtedness to our colleagues in the PS Linac Group for their essential contribution to the operation, the improvements and the measurements on the Linac.

References

[1] B. Vosicki, M. Buzic and A. Cheretakis
The Duoplasmatron Source for the CERN - PS Linac, 1966 Linear Accelerator Conference, Los Alamos.

[2] J. Huguenin, R. Dubois, G. Visconti, R. El-Bez
The New 500 keV Single-Gap Pre-injector for the CERN Proton Synchrotron Linac, 1966 Linear Accelerator Conference, Los Alamos.

[3] C.S. Taylor, D.J. Warner, F. Block and P. Têtu
Progress Report on the CERN - PS Linac, 1966 Linear Accelerator Conference, Los Alamos.

[4] J. Huguenin, U. Tallgren, M. Weiss,
Preliminary Study for a Higher Energy Pre-injector for the CERN - PS , this Conference.

[5] P. Lapostolle,
Bunching, this Conference.

[6] E. Boltezar, H.F. Malthouse and D.J. Warner
A 3 MeV Experimental Proton Linac, this Conference.

[7] R.L. Gluckstern
The Effect of Quadrupole Fringing Fields on Coupling in Linacs, 1966 Linear Accelerator Conference, Los Alamos.

[8] A. Chasman,
Numerical Calculation of Coupling Effects in a Low Energy Proton Linac, 1966 Linear Accelerator Conference, Los Alamos.

Figure Captions

Fig. 1 Magnetic field in the duoplasmatron

Fig. 2 Breakdown and deconditioning rates of the accelerating tube since April 1966.

Fig. 3 Demounting of accelerating tube.

Fig. 4 Interior view of accelerating tube (the shielding electrodes have been removed).

Fig. 5 Titanium alloy cathode.

Fig. 6 Craters around the cathode beam hole.

Fig. 7 Graphical representation of the effect on horizontal density of an aperture limitation in the vertical plane.

Fig. 8 Effect of bunching on 500 keV density.

Fig. 9 10 MeV Emittances at end of Tank III for two separated 10 emittances drifted through Tank II and III.

Fig. 10 50 MeV Emittances at end of Tank III for two separated 10 MV emittances.

Fig. 11 Tank I RF field variation in the presence of beam (10 μs/cm).

Fig. 12 Time derivative of Tank I RF field for the conditions of Fig. 11 (10 μs/cm).

Fig. 13 RF pulse in Tank I with compensation (50 μs/cm).

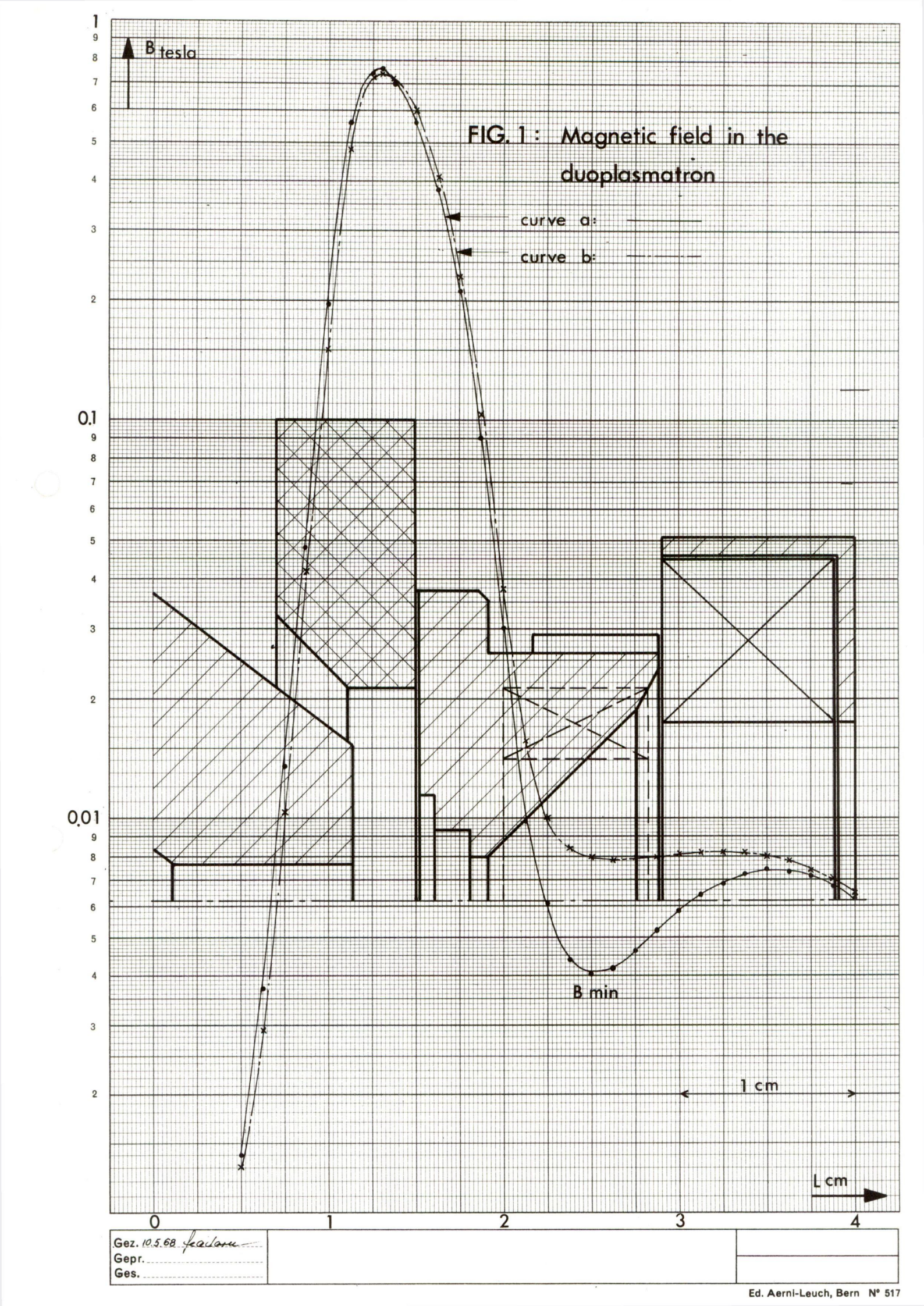

Gez. 10.5.68 Jeadam
Gepr.
Ges.

Ed. Aerni-Leuch, Bern N° 517

FIG. 2: Breakdown rate and deconditioning rate of the accelerating tube since april 1966

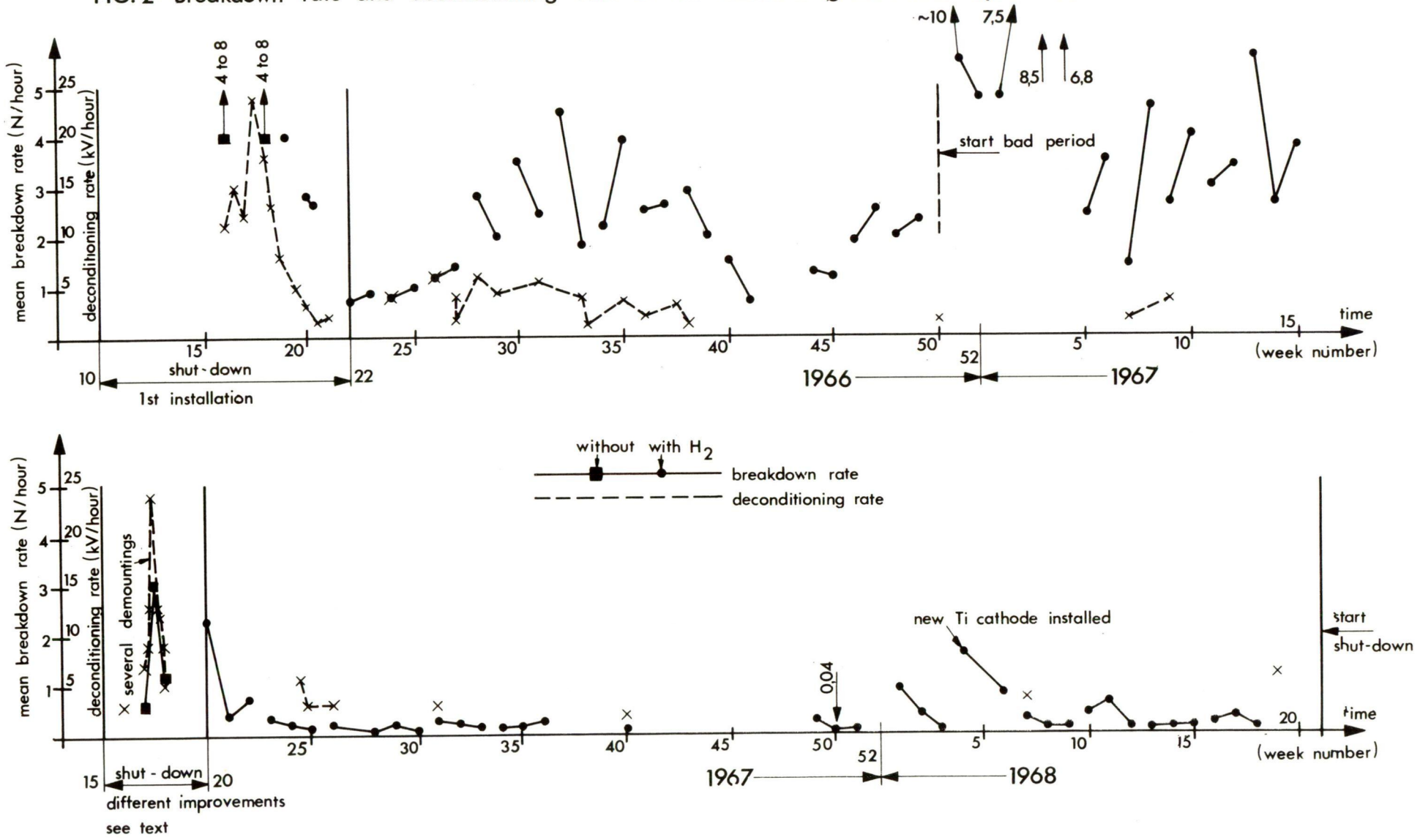

22.5.68

FIG. 3: Demounting of accelerating tube

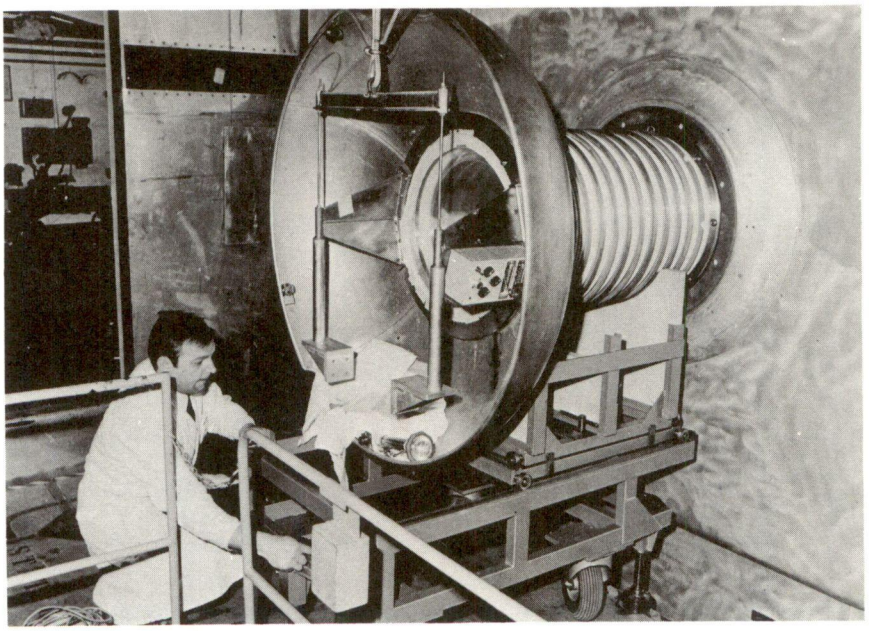

FIG. 4: Interior view of accelerating tube (the shielding electrodes have been removed)

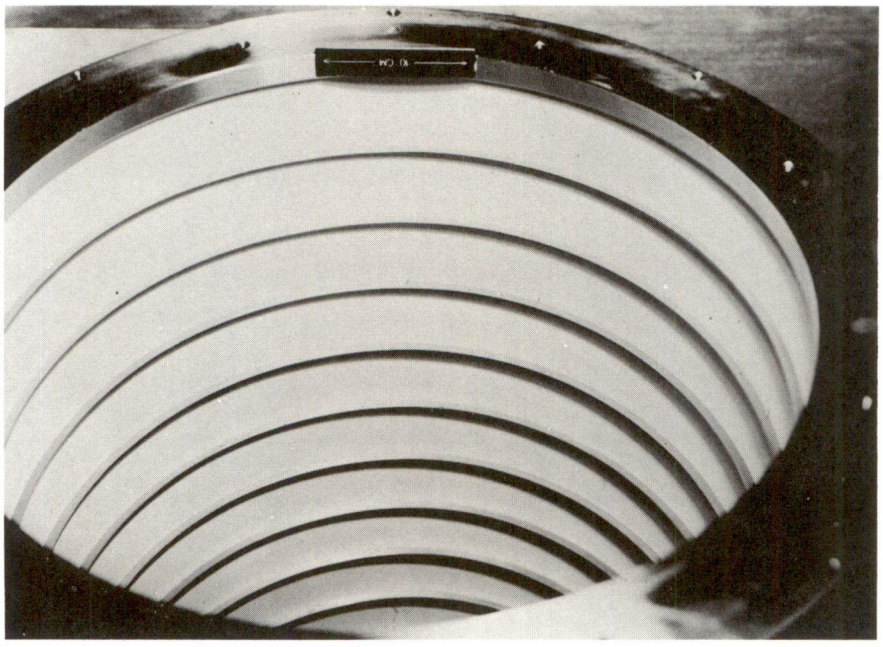

FIG. 5: Titanium alloy cathode

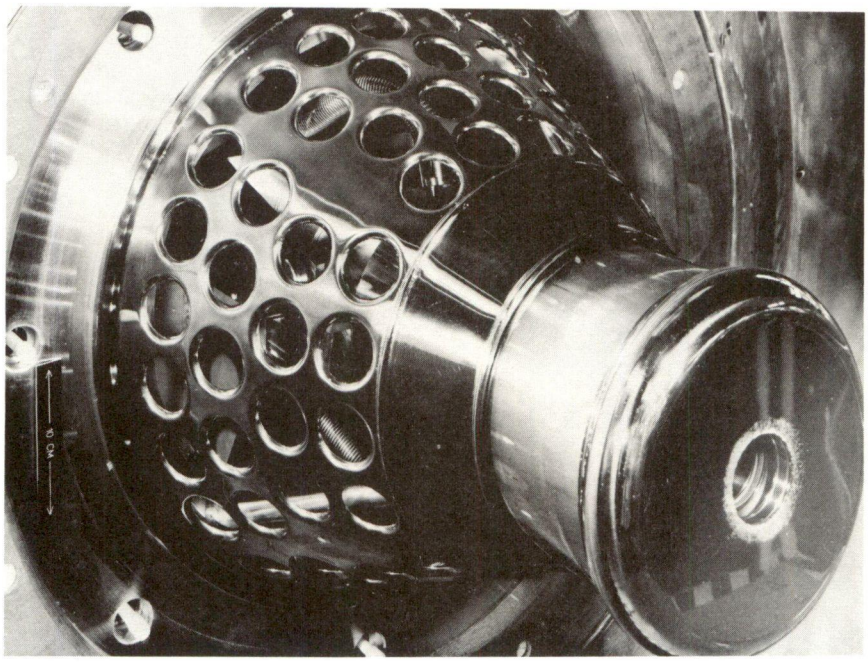

FIG. 6: Craters around the cathode beam hole

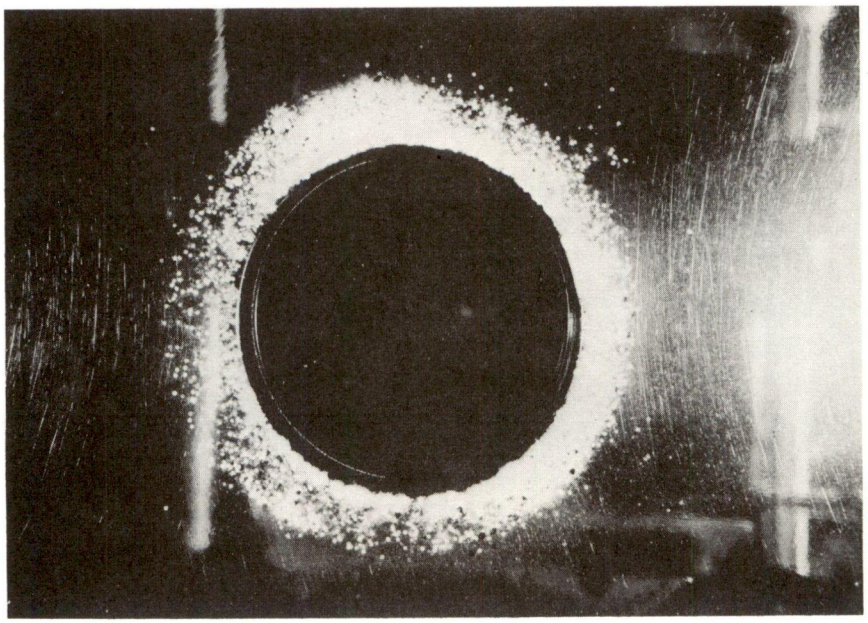

FIG. 7: Graphical representation of the effect on horizontal density of an operture in the vertical plane.

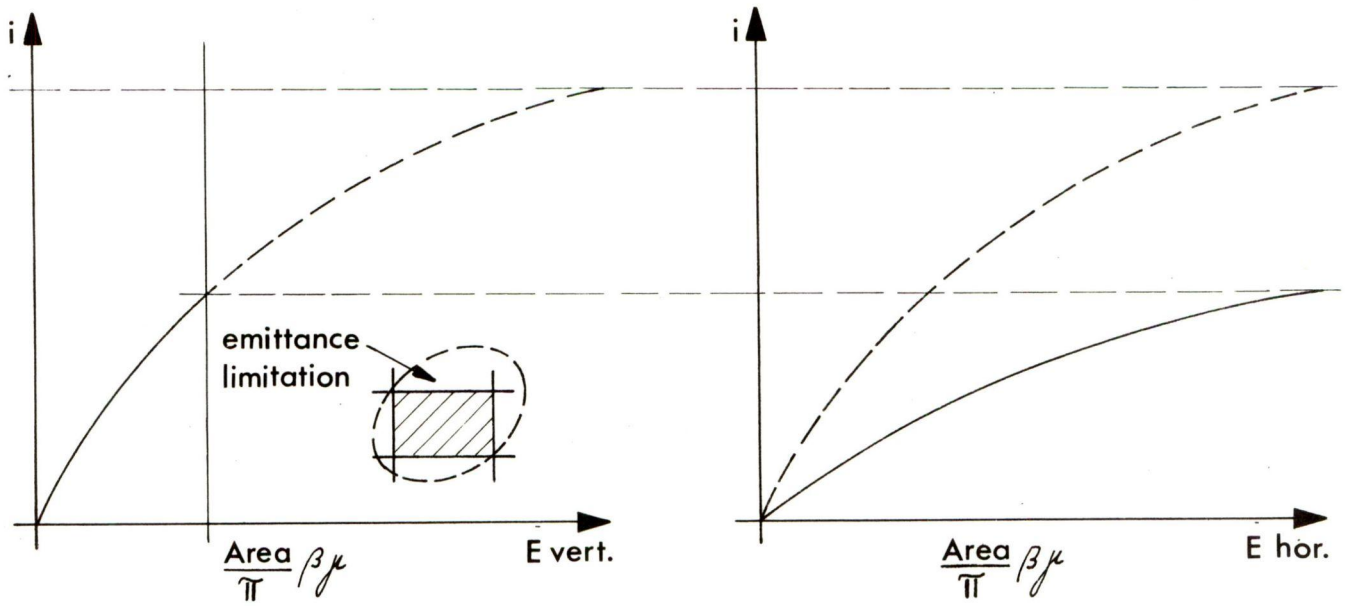

21.5.68 Headam

FIG. 8: Effect of bunching on 500 keV density

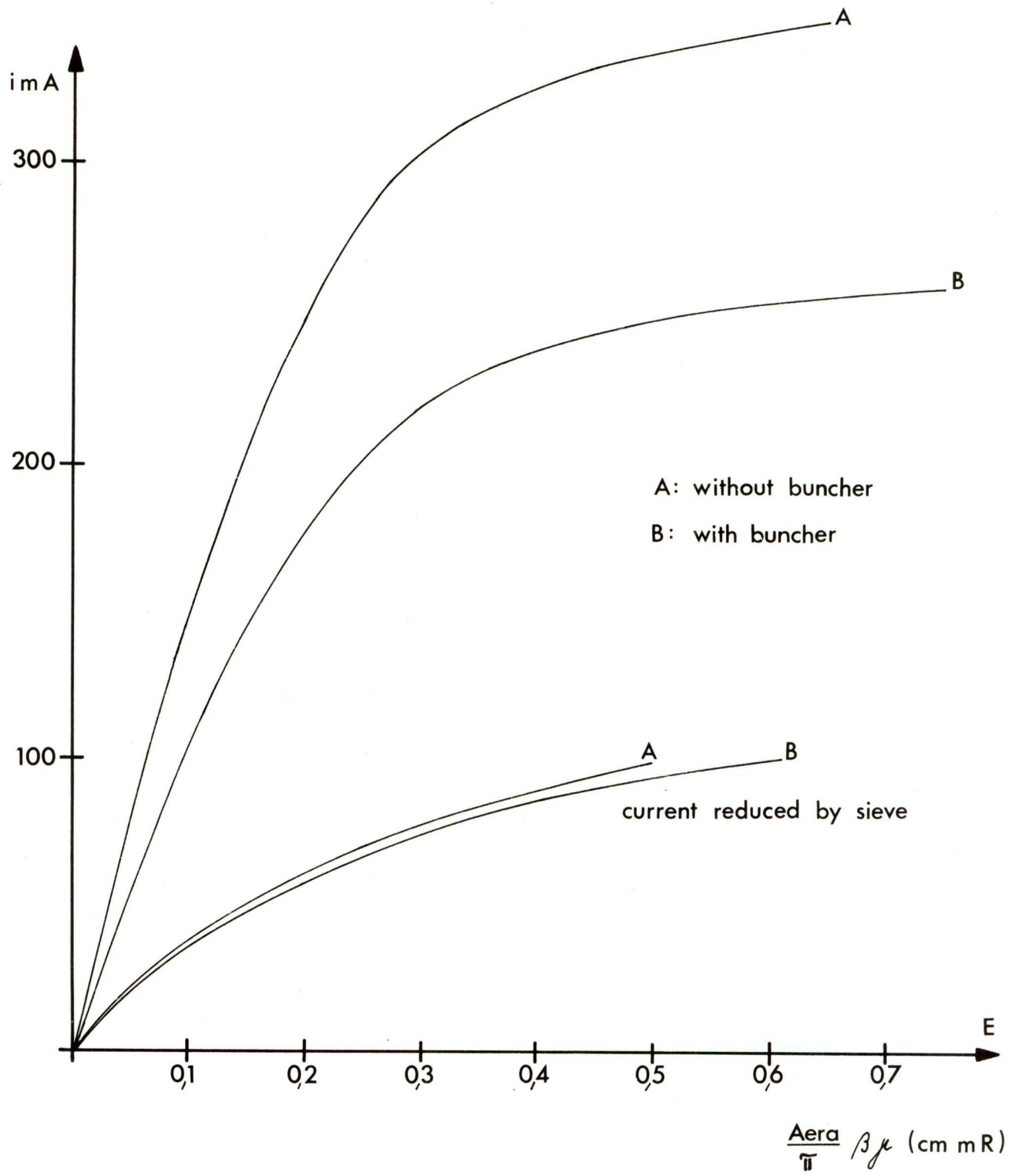

20.5.68

FIG. 9: 10 MeV emittances at end of tank III for two seperated 10 MeV emittances driffed through tanks II and III

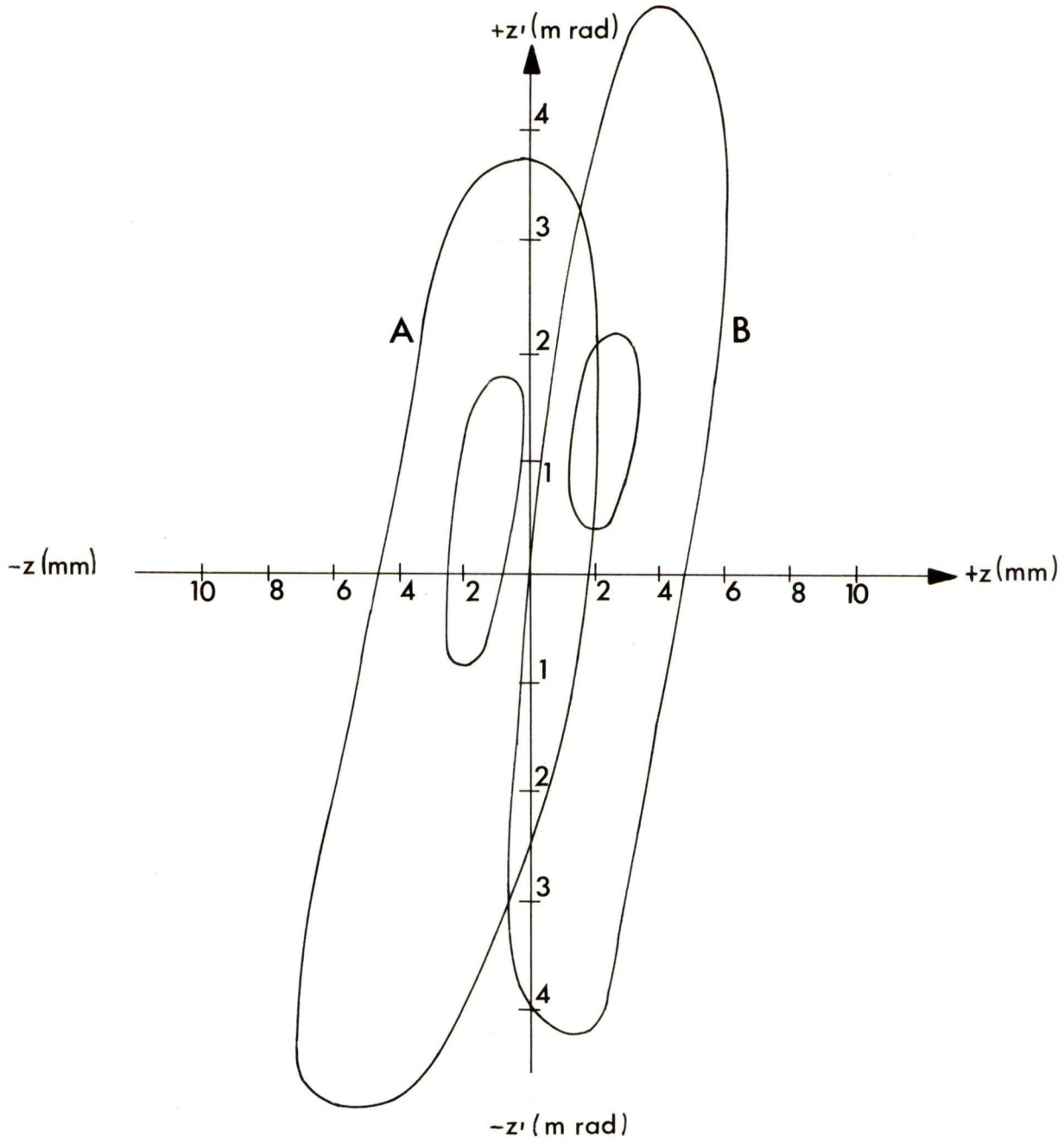

separated input emittances at 10 MeV produced by:

A – a 5 mm wide obstruction

B – a 5 mm wide slit

20.5.68 Headon

FIG. 10: 50 MeV emittances at end of tank III for two separated 10 MeV emittances

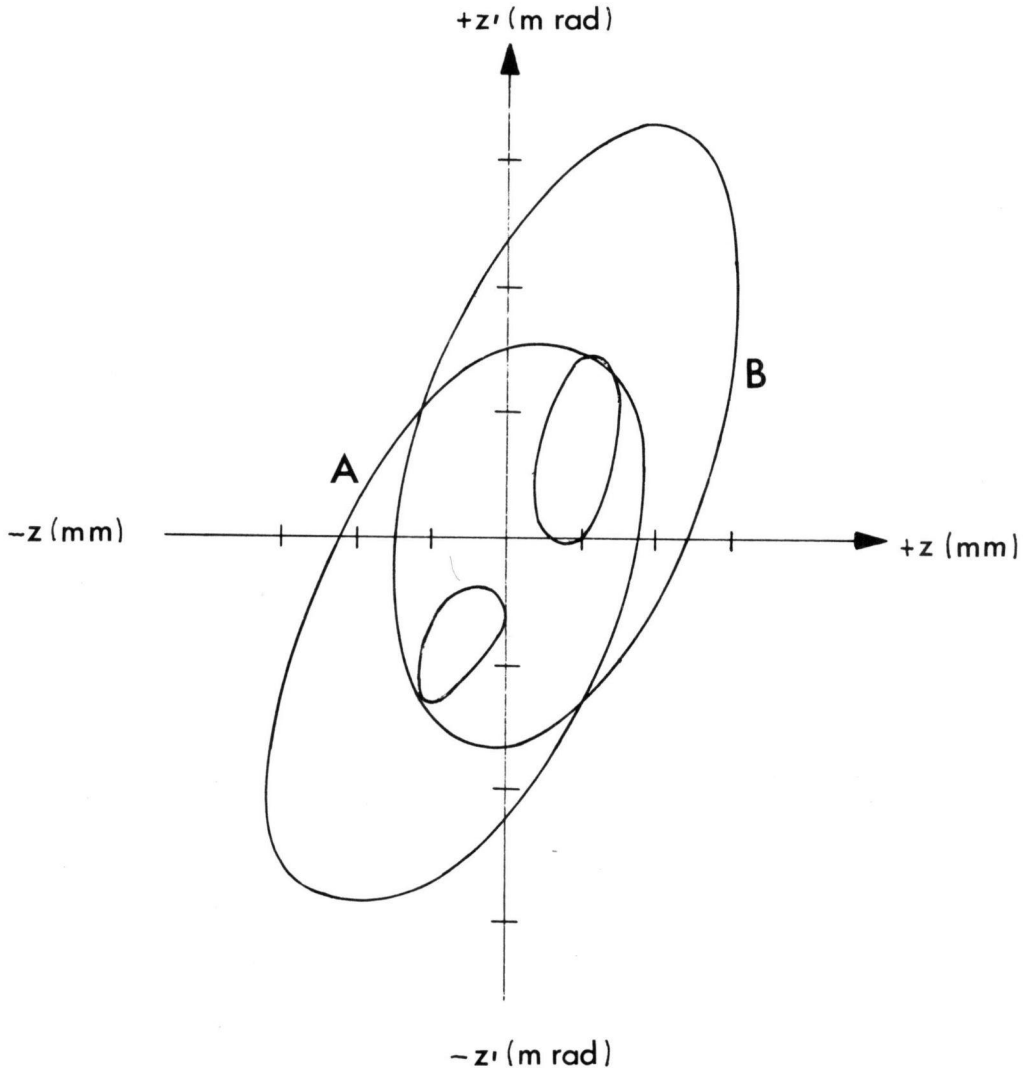

separated emittances produced as in Fig. 8

21.5.68 Hadone

FIG. 11: Tank I R.F. field variation in the presence of beam (10 μs/cm)

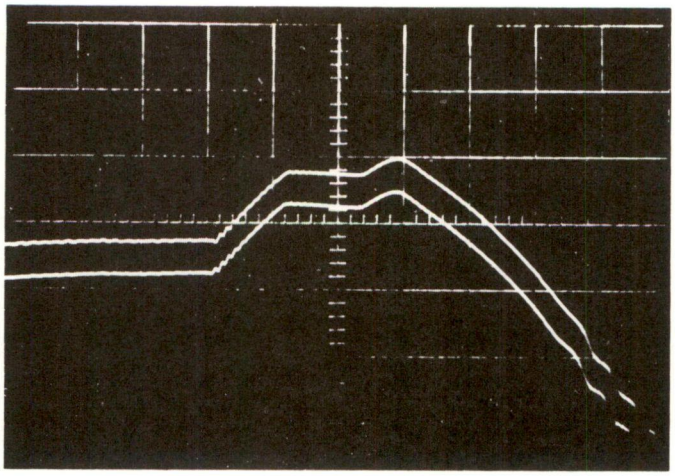

FIG. 12: Time derivative of tank I R.F. field for the conditions of Fig. 11. (10μs/cm)

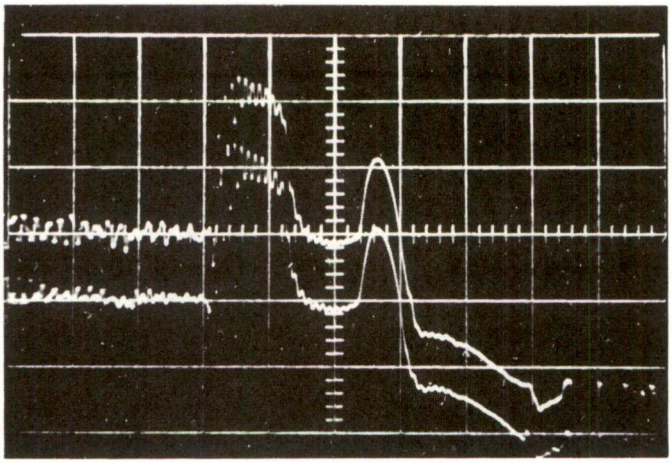

FIG. 13: R.F. pulse in tank I with compensation. (50 u s/cm)